

## **Resonant modes in strain-induced graphene superlattices**

F. M. D. Pellegrino,<sup>1,2</sup> G. G. N. Angilella,<sup>1,2,3,4</sup> and R. Pucci<sup>1,2</sup>

<sup>1</sup>*Dipartimento di Fisica e Astronomia, Università di Catania, Via S. Sofia, 64, I-95123 Catania, Italy*

<sup>2</sup>*CNISM, UdR di Catania, I-95123 Catania, Italy*

<sup>3</sup>*Scuola Superiore di Catania, Università di Catania, Via Valdisavoia, 9, I-95123 Catania, Italy*

<sup>4</sup>*INFN, Sezione di Catania, I-95123 Catania, Italy*

(Received 20 March 2012; published 7 May 2012)

---

Journal Club, May 15th 2012

Gerson J. Ferreira

*Department of Physics, University of Basel, Switzerland*

# Direct Observation of Interband Spin-Orbit Coupling in a Two-Dimensional Electron System

Hendrik Bentmann,<sup>1,2</sup> Samir Abdelouahed,<sup>3</sup> Mattia Mulazzi,<sup>1,2</sup> Jürgen Henk,<sup>4</sup> and Friedrich Reinert<sup>1,2</sup>

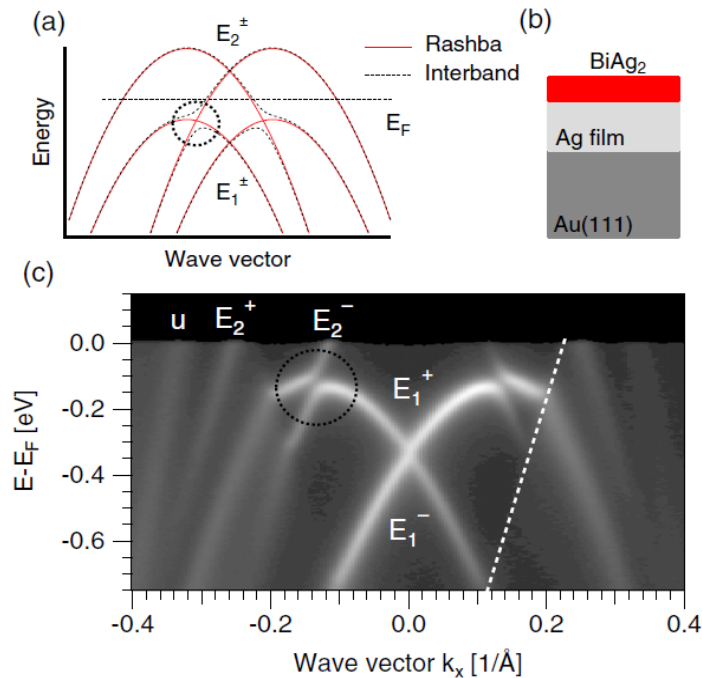
<sup>1</sup>*Experimentelle Physik VII and Röntgen Research Center for Complex Materials (RCCM),  
Universität Würzburg Am Hubland, D-97074 Würzburg, Germany*

<sup>2</sup>*Karlsruhe Institute of Technology KIT, Gemeinschaftslabor für Nanoanalytik, D-76021 Karlsruhe, Germany*

<sup>3</sup>*Texas A&M University at Qatar, P. O. Box 23874, Doha, Qatar*

<sup>4</sup>*Institut für Physik—Theoretische Physik, Martin-Luther-Universität Halle-Wittenberg, D-06099 Halle (Saale), Germany*  
(Received 16 January 2012; published 7 May 2012)

We report the direct observation of interband spin-orbit (SO) coupling in a two-dimensional (2D) surface electron system, in addition to the anticipated Rashba spin splitting. Using angle-resolved photoemission experiments and first-principles calculations on Bi-Ag-Au heterostructures, we show that the effect strongly modifies the dispersion as well as the orbital and spin character of the 2D electronic states, thus giving rise to considerable deviations from the Rashba model. The strength of the interband SO coupling is tuned by the thickness of the thin film structures.



PRL 99, 076603 (2007)

PHYSICAL REVIEW LETTERS

week ending  
17 AUGUST 2007

## Spin-Orbit Interaction in Symmetric Wells with Two Subbands

Esmerindo Bernardes,<sup>1</sup> John Schliemann,<sup>2,3</sup> Minchul Lee,<sup>3</sup> J. Carlos Egues,<sup>1,3,4</sup> and Daniel Loss<sup>3,4</sup>

PHYSICAL REVIEW B 78, 155313 (2008)

## Intersubband-induced spin-orbit interaction in quantum wells

Rafael S. Calsaverini,<sup>1</sup> Esmerindo Bernardes,<sup>1,\*</sup> J. Carlos Egues,<sup>1,†</sup> and Daniel Loss<sup>2</sup>

- Changes in the hopping due to modulation in the bond length;
- Low energy Hamiltonian:

$$H = \hbar v_F \mathcal{U}^\dagger(\theta) \tilde{\sigma} \cdot \mathbf{q} \mathcal{U}(\theta),$$

- $\mathbf{q}$ : wave-vector displacement from the shifted Dirac cones:

$$\mathbf{q}_{DA} = \pm [\kappa_0 \varepsilon (1 + \nu) \cos(2\theta), -\kappa_0 \varepsilon (1 + \nu) \sin(2\theta)]^\top$$

$$\begin{aligned} \theta = 0 & : \text{zigzag} \\ \theta = \pi/2 & : \text{armchair} \end{aligned}$$

$$\tilde{\sigma}_i = (1 - \lambda_i \varepsilon) \sigma_i$$

accounts for the deformation of the Fermi velocity

$$\kappa_0 = (a/2t) |\partial t / \partial a| \approx 1.6$$

derivative of the hopping parameter  $t$

$\nu=1.4$ : Poisson's ratio

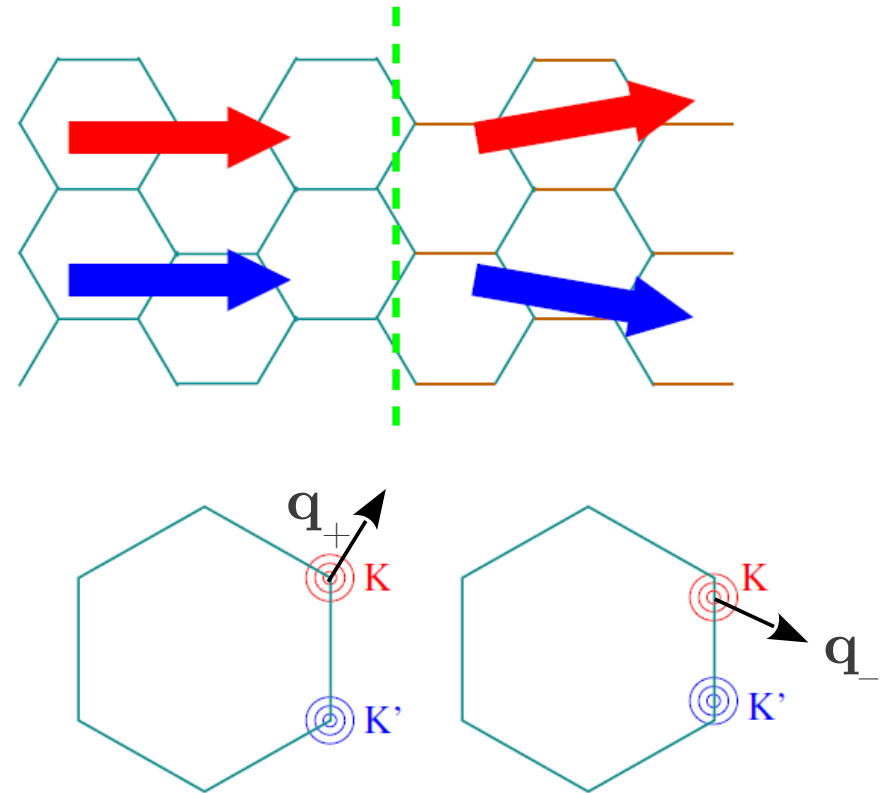


FIG. 29. (Color online) Gauge field induced by a simple elastic strain. Top: the hopping along the horizontal bonds is assumed to be changed on the right-hand side of the graphene lattice, defining a straight boundary between the unperturbed and perturbed regions (dashed line). Bottom: the modified hopping acts like a constant gauge field, which displaces the Dirac cones in opposite directions at the  $K$  and  $K'$  points of the Brillouin zone. The conservation of energy and momentum parallel to the boundary leads to a deflection of electrons by the boundary.

[Castro-Neto, *et al.*, RMP **81**, 109 (2009)]

- Changes in the hopping due to modulation in the bond length;
- Low energy Hamiltonian:

$$H = \hbar v_F \mathcal{U}^\dagger(\theta) \tilde{\sigma} \cdot \mathbf{q} \mathcal{U}(\theta),$$

- $\mathbf{q}$ : wave-vector displacement from the shifted Dirac cones:

$$\mathbf{q}_{DA} = \pm [\kappa_0 \varepsilon (1 + \nu) \cos(2\theta), -\kappa_0 \varepsilon (1 + \nu) \sin(2\theta)]^\top$$

$$\begin{aligned} \theta = 0 & : \text{zigzag} \\ \theta = \pi/2 & : \text{armchair} \end{aligned}$$

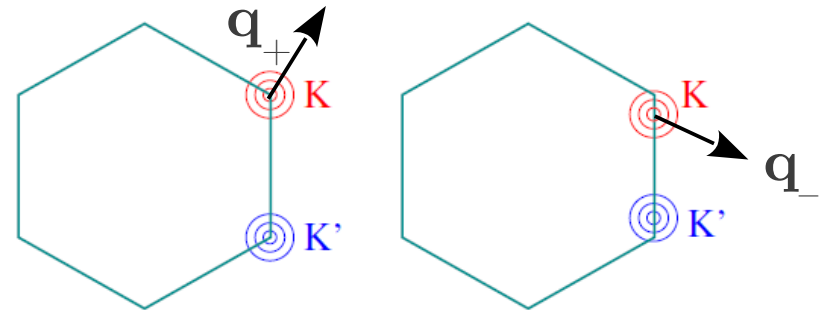
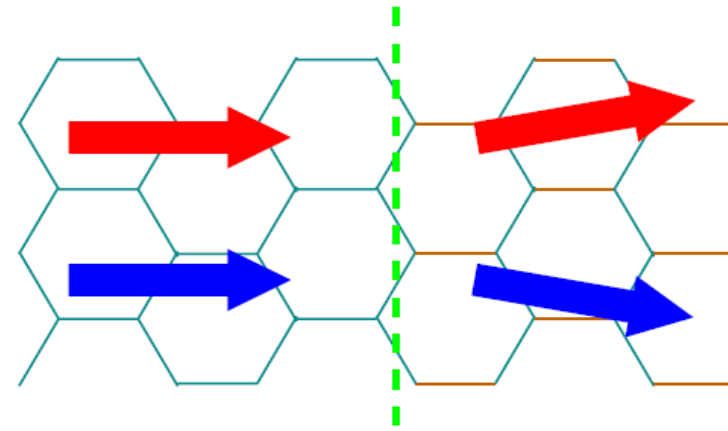
$$\tilde{\sigma}_i = (1 - \lambda_i \varepsilon) \sigma_i$$

accounts for the deformation of the Fermi velocity

$$\kappa_0 = (a/2t) |\partial t / \partial a| \approx 1.6$$

derivative of the hopping parameter  $t$

$$\nu = 1.4: \text{Poisson's ratio}$$



- Strain-induced modification of the work function (*next-nearest-neighbor hopping*)

$$\Phi = \frac{3}{2} (1 - \nu) \sqrt{3} a \left. \frac{dV_{pp\pi}(\ell)}{d\ell} \right|_{\ell = \sqrt{3}a} \quad \varepsilon \approx 1.7 \text{ eV} \times \varepsilon$$

# Strain & Electrostatic Potential modulation: superlattice

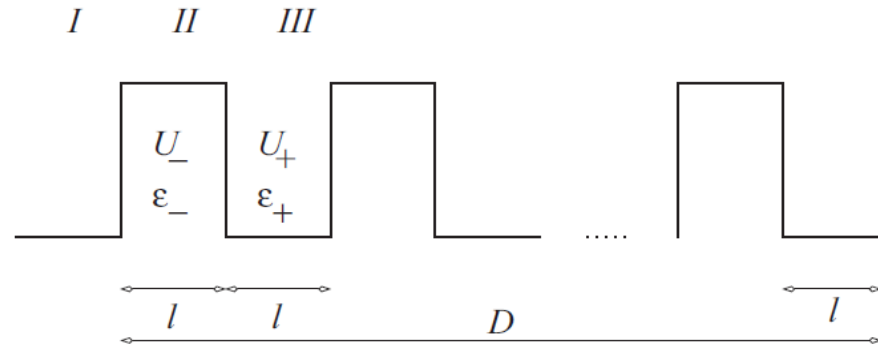


FIG. 1. Schematic plot of the superlattice of  $N$  identical barriers, with  $\ell$  denoting both each barrier's width and the interbarrier separation, while  $D = 2N\ell$ . Subscript  $-$  refers to the region within a barrier (labeled II), while subscript  $+$  refers to the interbarrier region (labeled I and III).

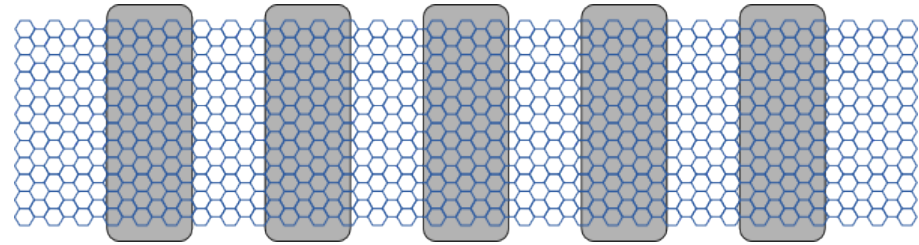
- Piecewise constant profile;
- Transmission via Transfer Matrix;
  - Chebyshev identity for  $M^N$
- $U$  is always zero in this paper...  
(left over from other papers; copy/paste)

# Transfer Matrix

[GJF, Leuenberger, Loss, Egues, PRB **84**, 125453 (2011)]

- Considering only the electrostatic potential here;
  - Since strain profile is piecewise constant, the idea is the same

$$\psi_{j,n}(x,y) = e^{ik_n y} \varphi_j(x)$$



$$\varphi_j(x) = M_j(x) \phi_j$$

$$\phi_j^T = (\alpha_j \quad \beta_j)^T$$

Defining the spinor in a matrix notation

$$M_j(x) = \begin{pmatrix} e^{ik_x^{(j)} x} & e^{-ik_x^{(j)} x} \\ s_j e^{ik_x^{(j)} x + i\theta_{j,n}} & -s_j e^{-ik_x^{(j)} x - i\theta_{j,n}} \end{pmatrix}$$

Continuity of the spinor along the interfaces

$$\varphi_j(x_{j,j+1}) = \varphi_{j+1}(x_{j,j+1})$$

Transfer matrix connects the source and drain spinor coefficients

$$T_M = \prod_j M_j^{-1}(x_{j,j+1}) M_{j+1}(x_{j,j+1}).$$

If all barriers are equivalent:

$$T_M = \tilde{M}^N = [M_j^{-1} M_{j+1}]^N$$

Chebyshev identity:  
Nth power of a 2x2 matrix

$$\mathbf{P}^N = \mathbf{P} U_{N-1}(\xi) - \mathbf{I} U_{N-2}(\xi)$$

$$U_N(\xi) = \frac{\sin(N+1)\gamma}{\sin \gamma}$$

- Effects of strain regarding the ballistic transport, no modulation/superlattice

$$\sigma = \frac{D}{W} G, \quad \begin{array}{l} D \mapsto D_{\text{eff}} \equiv \xi D, \\ E \mapsto E_{\text{eff}} \equiv \zeta E, \end{array}$$

$$\xi = \frac{1 - \lambda_y \varepsilon}{1 - \lambda_x \varepsilon}$$

$$\zeta = \frac{1}{1 - \lambda_y \varepsilon}$$

$$\sigma(D, E) = \xi^{-1} \sigma^{(0)}(D_{\text{eff}}, E_{\text{eff}})$$

- Effects of strain regarding the ballistic transport, no modulation/superlattice

$$\sigma = \frac{D}{W} G,$$

$$D \mapsto D_{\text{eff}} \equiv \xi D,$$

$$E \mapsto E_{\text{eff}} \equiv \zeta E,$$

$$\xi = \frac{1 - \lambda_y \varepsilon}{1 - \lambda_x \varepsilon}$$

$$\zeta = \frac{1}{1 - \lambda_y \varepsilon}$$

$$\sigma(D, E) = \xi^{-1} \sigma^{(0)}(D_{\text{eff}}, E_{\text{eff}})$$

Minimum conductivity:

$$\lim_{E \rightarrow 0} \sigma(D, E) = \frac{1}{\xi} \frac{4e^2}{\pi h}$$

Asymptotic limit:

$$\sigma_{\infty}(E) = \frac{4e^2}{h} \frac{D|E|}{4} \zeta$$



- Effects of strain regarding the ballistic transport, no modulation/superlattice

$$\sigma = \frac{D}{W} G,$$

$$D \mapsto D_{\text{eff}} \equiv \xi D,$$

$$E \mapsto E_{\text{eff}} \equiv \zeta E,$$

$$\xi = \frac{1 - \lambda_y \varepsilon}{1 - \lambda_x \varepsilon}$$

$$\zeta = \frac{1}{1 - \lambda_y \varepsilon}$$

$$\sigma(D, E) = \xi^{-1} \sigma^{(0)}(D_{\text{eff}}, E_{\text{eff}})$$

Minimum conductivity:

$$\lim_{E \rightarrow 0} \sigma(D, E) = \frac{1}{\xi} \frac{4e^2}{\pi h}$$

Asymptotic limit:

$$\sigma_{\infty}(E) = \frac{4e^2}{h} \frac{D|E|}{4} \zeta$$

Frequency of the oscillations:

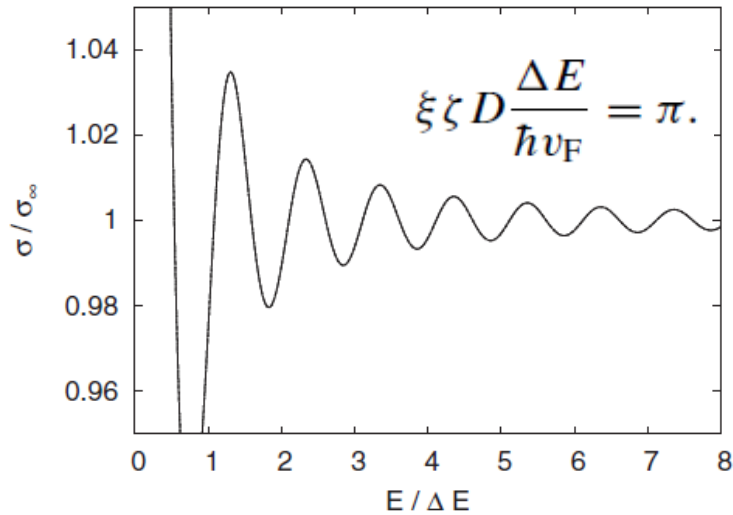


FIG. 5. Conductivity across a graphene strip ( $D = 100$  nm) normalized to asymptotic large-energy behavior, Eq. (31), vs energy scaled to the pseudoperiod, Eq. (32). Actually shown are four curves, all collapsing into a single one, corresponding to strain applied along the armchair direction ( $\theta = \pi/2$ ), with  $\varepsilon = 0.03, 0.05, 0.10, 0.15$ .

Fano factor

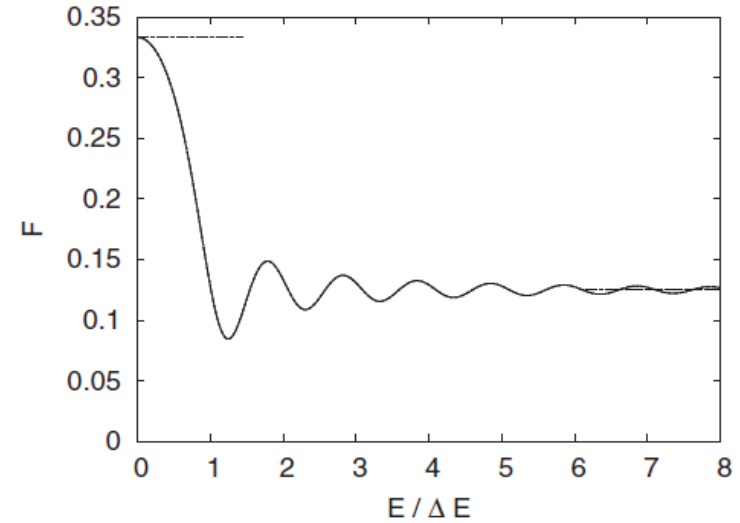


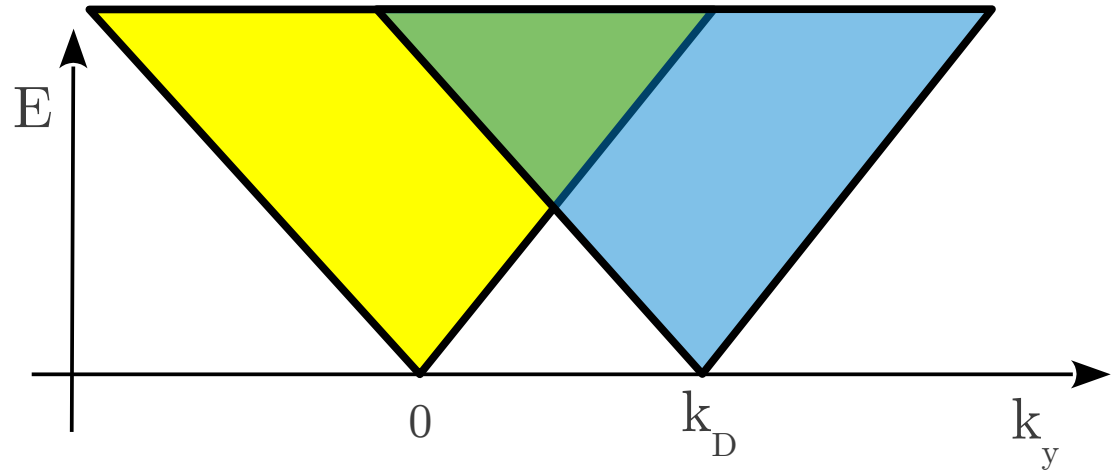
FIG. 6. Fano factor for ballistic transport across a graphene strip. All parameters are as in Fig. 5. Dashed lines represent the universal low- and large-energy asymptotic values,  $F(0) = \frac{1}{3}$  and  $F_{\infty} = \frac{1}{8}$ , respectively.

# Transport: single barrier

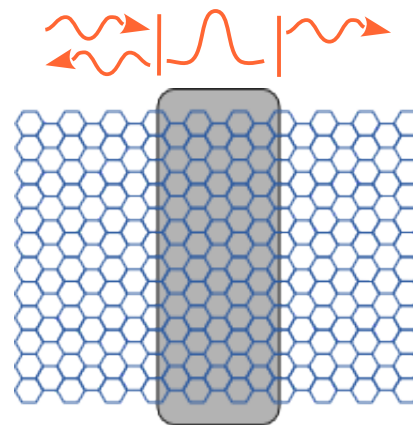
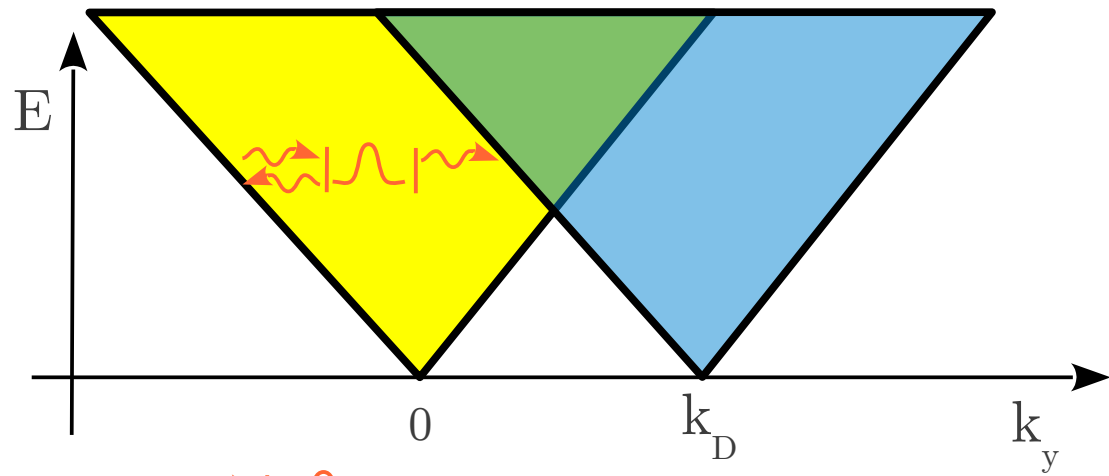
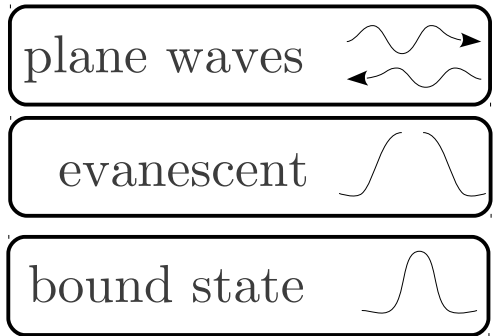
plane waves 

evanescent 

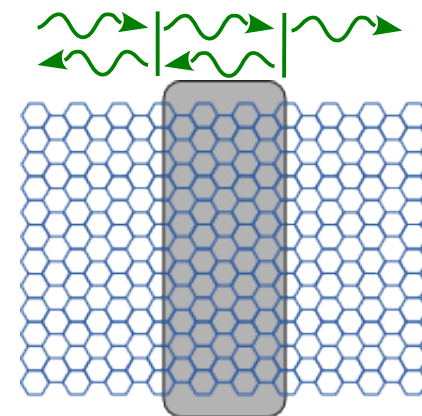
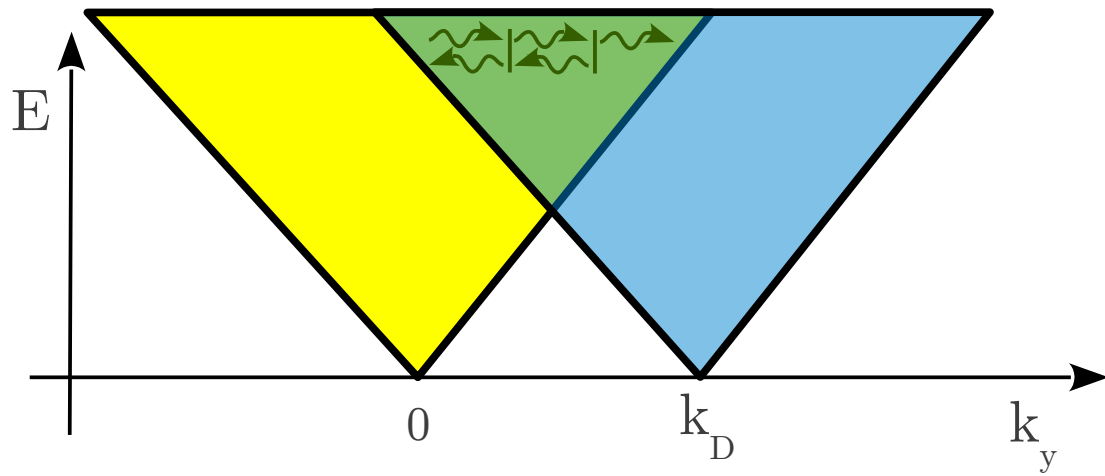
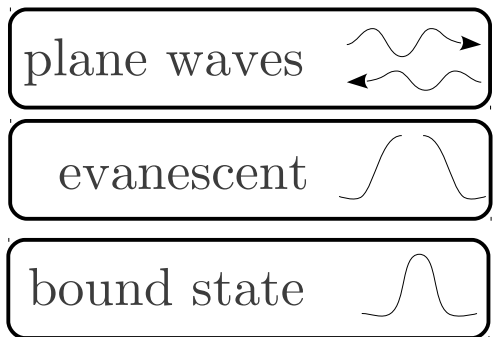
bound state 



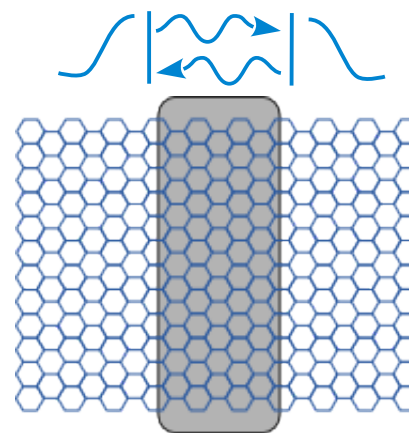
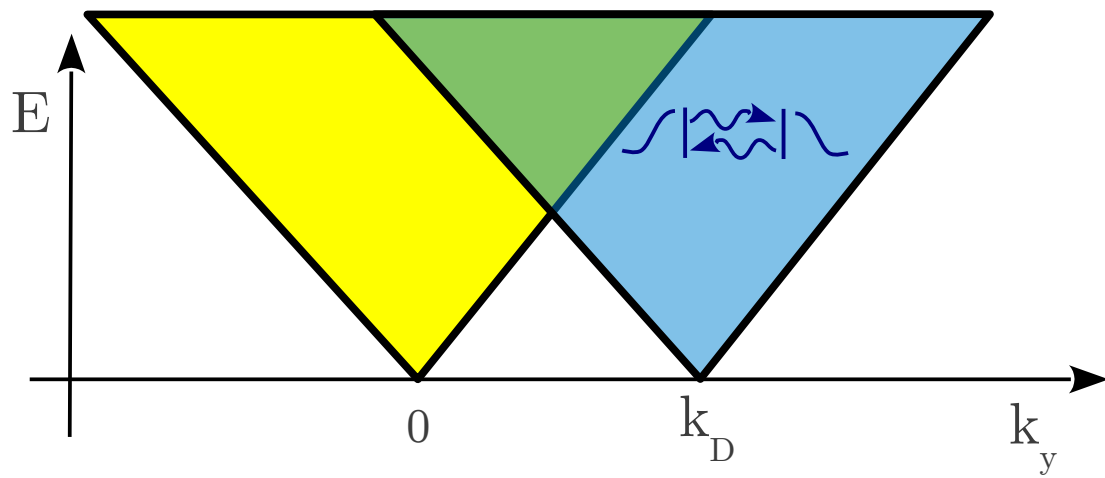
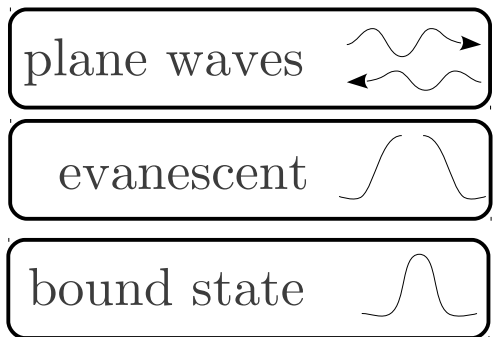
# Single "barrier"



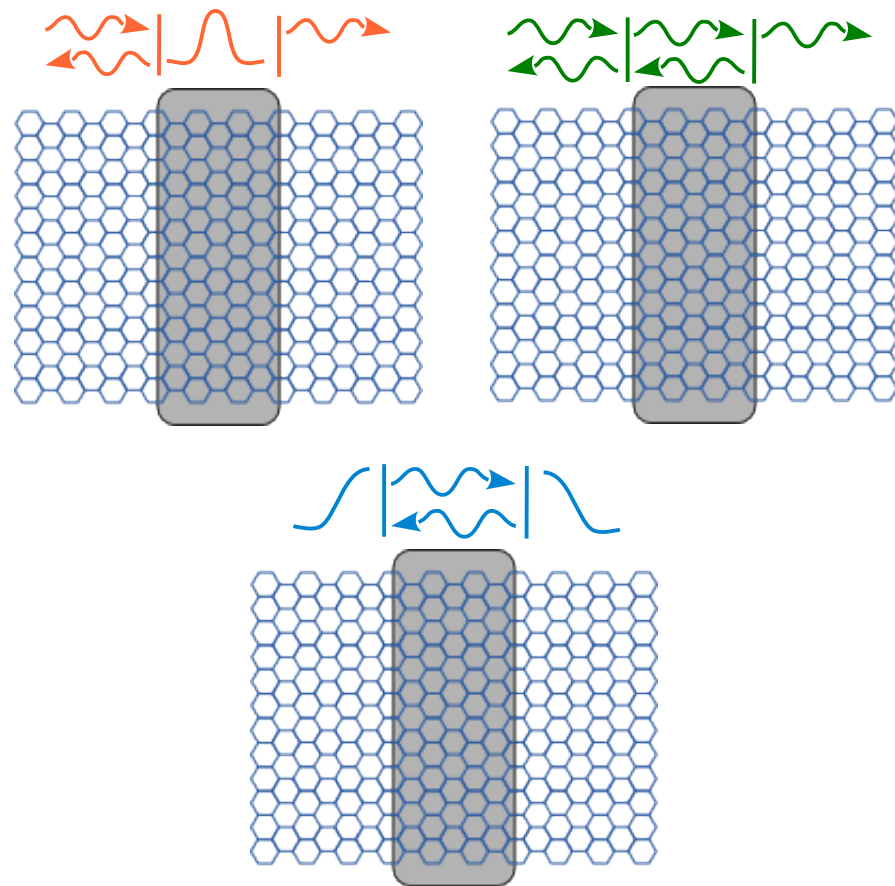
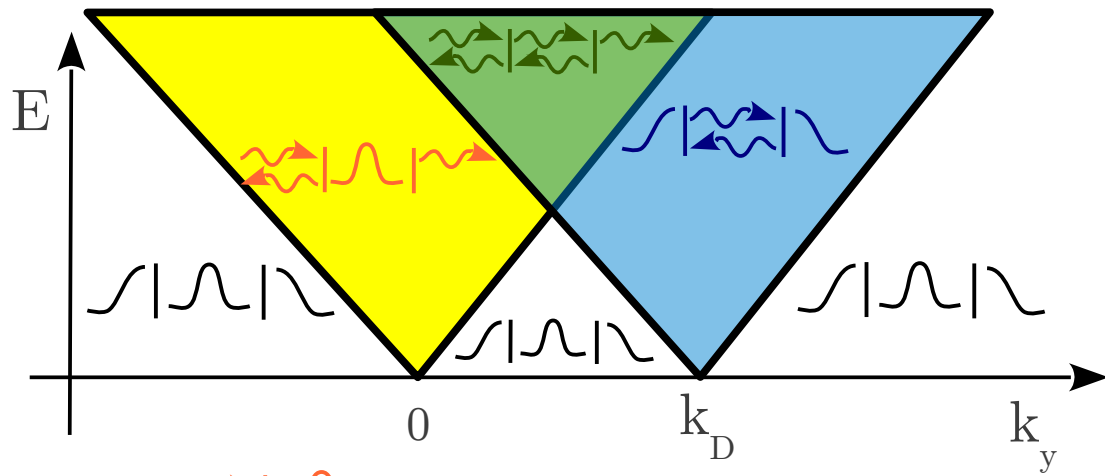
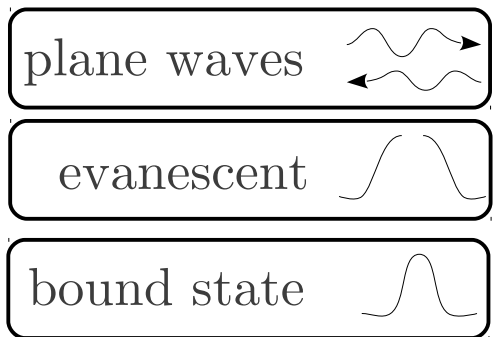
# Single "barrier"



# Single "barrier"



# Single "barrier"



# Single “barrier”

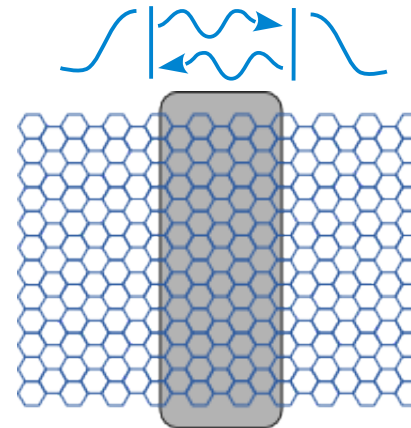
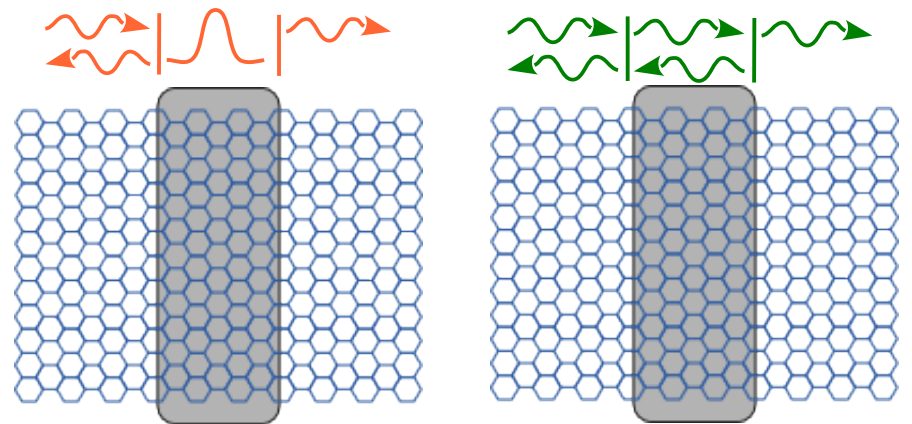
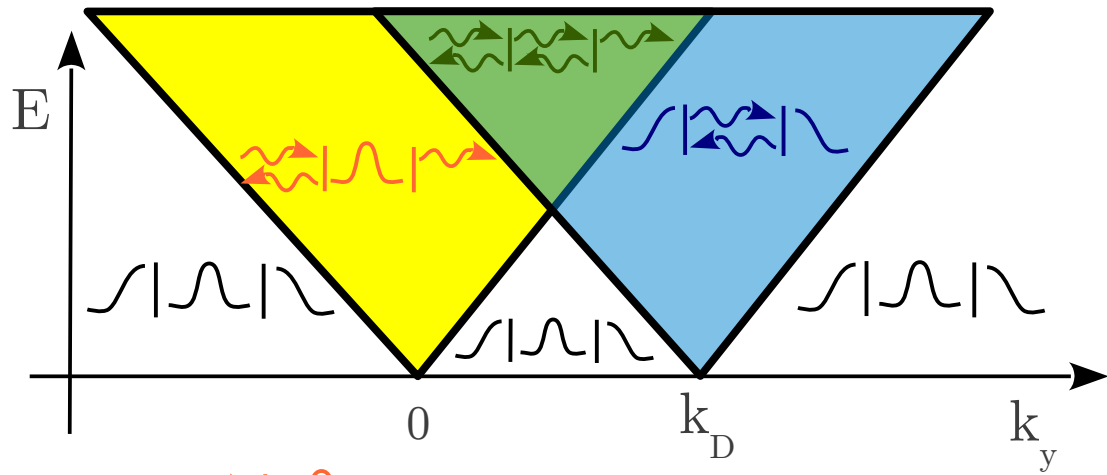
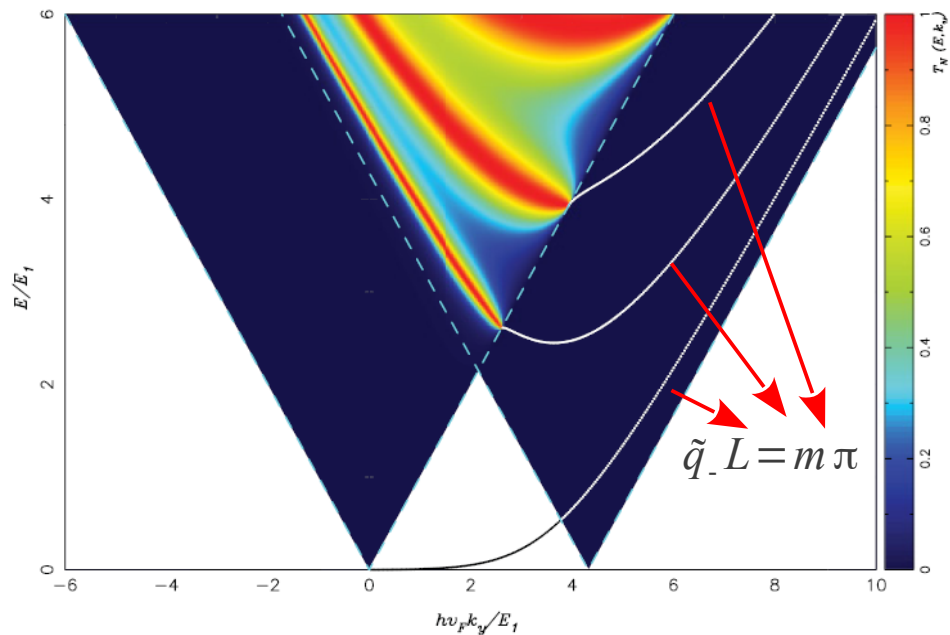
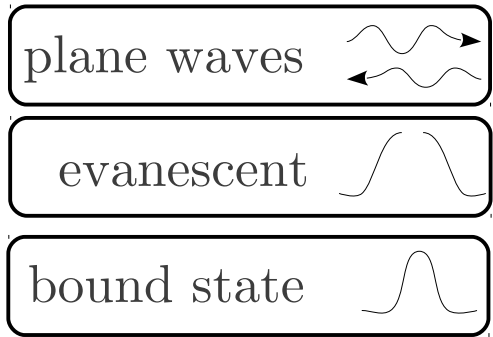


FIG. 2. (Color online) Single-electron transmission  $T_1(E, k_y)$ , Eq. (5) across a single barrier ( $N = 1$ ,  $\ell = 25$  nm), as a function of scaled transverse wave vector  $\hbar v_F k_y / E_1$  and scaled energy  $E / E_1$ , Eq. (6), with  $E_1 \approx 40$  meV. Here, strain is applied along the armchair direction,  $\theta = \pi/2$ , and we set  $\varepsilon_- = 0.02$ ,  $\varepsilon_+ = 0$ , and  $U_{\pm} = 0$ . Cyan dashed lines delimit cones corresponding to the (deformed) Dirac cones outside (left cone) and within (right cone) the barrier (regions I + III and II, respectively, in Fig. 1). Solid lines outside the left Dirac cone correspond to bound modes.

# $N=5$ “barriers”: minibands, and hybridization of bound states

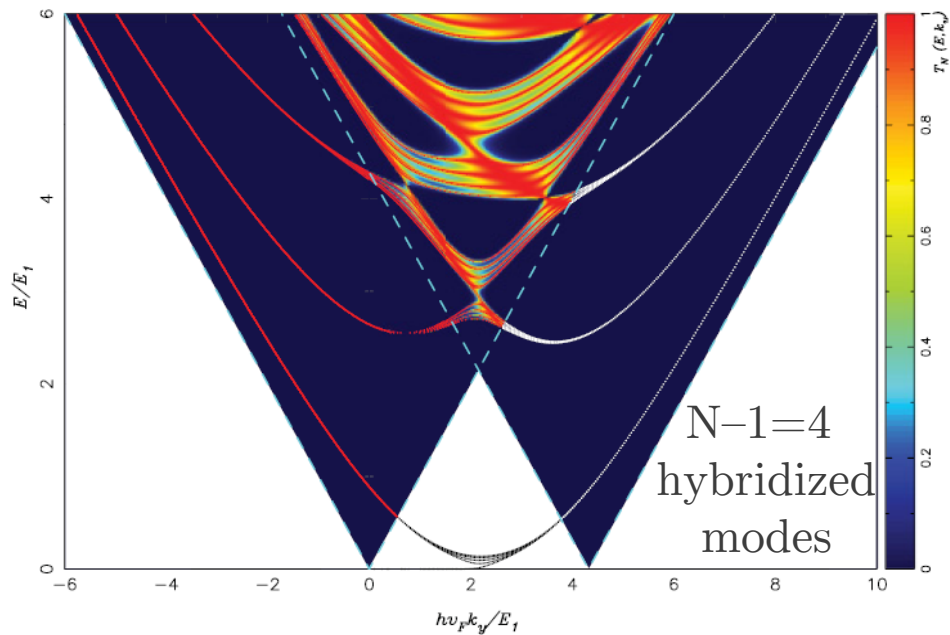
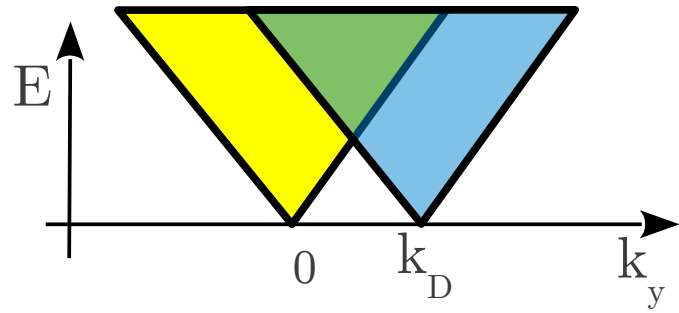


FIG. 3. (Color online) Single-electron transmission  $T_5(E, k_y)$ , Eq. (5) across a superlattice of  $N = 5$  identical barriers (Fig. 1), as a function of scaled transverse wave vector  $\hbar v_F k_y / E_1$  and scaled energy  $E/E_1$ , Eq. (6). All other parameters are as in Fig. 2. Red lines outside the right cone correspond to resonant modes.



# $N=5$ “barriers”: minibands, and hybridization of bound states

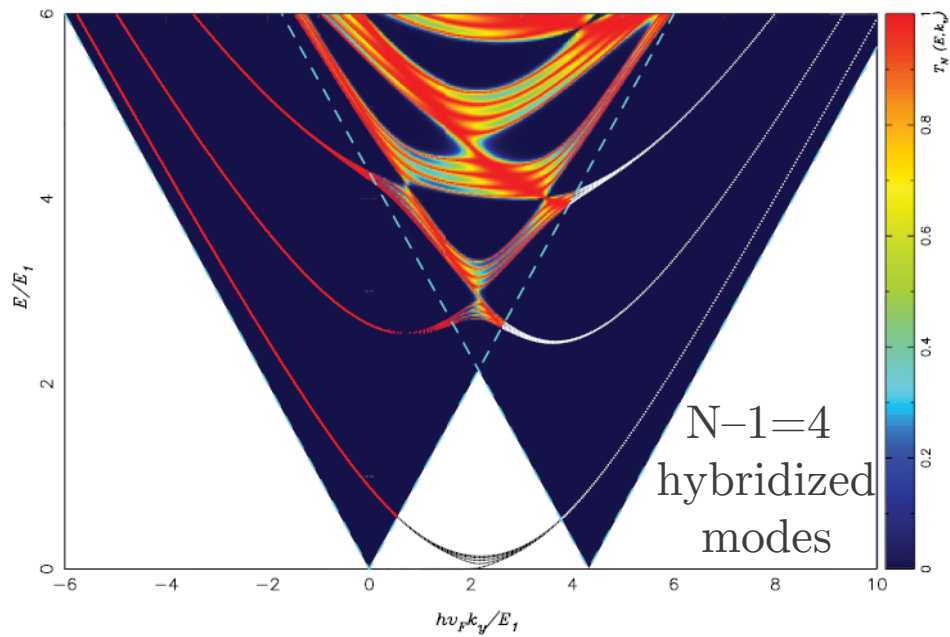
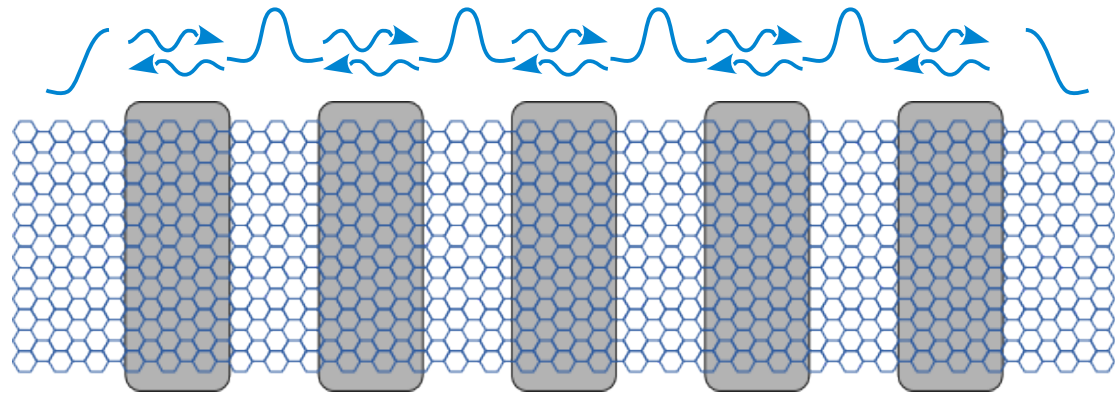
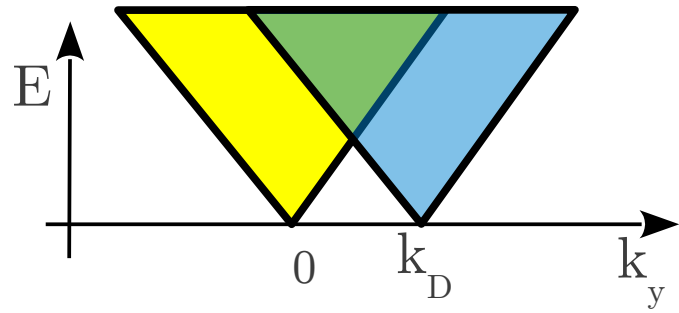


FIG. 3. (Color online) Single-electron transmission  $T_5(E, k_y)$ , Eq. (5) across a superlattice of  $N = 5$  identical barriers (Fig. 1), as a function of scaled transverse wave vector  $\hbar v_F k_y / E_1$  and scaled energy  $E / E_1$ , Eq. (6). All other parameters are as in Fig. 2. Red lines outside the right cone correspond to resonant modes.

# $N=5$ “barriers”: minibands, and hybridization of bound states

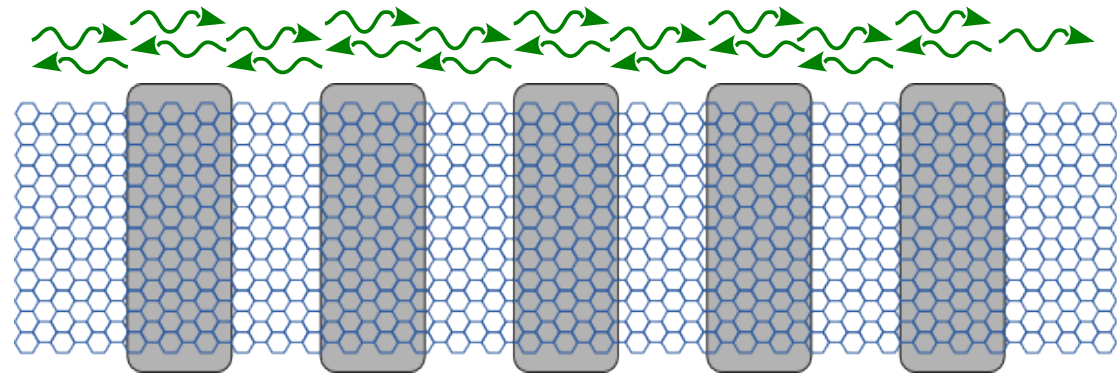
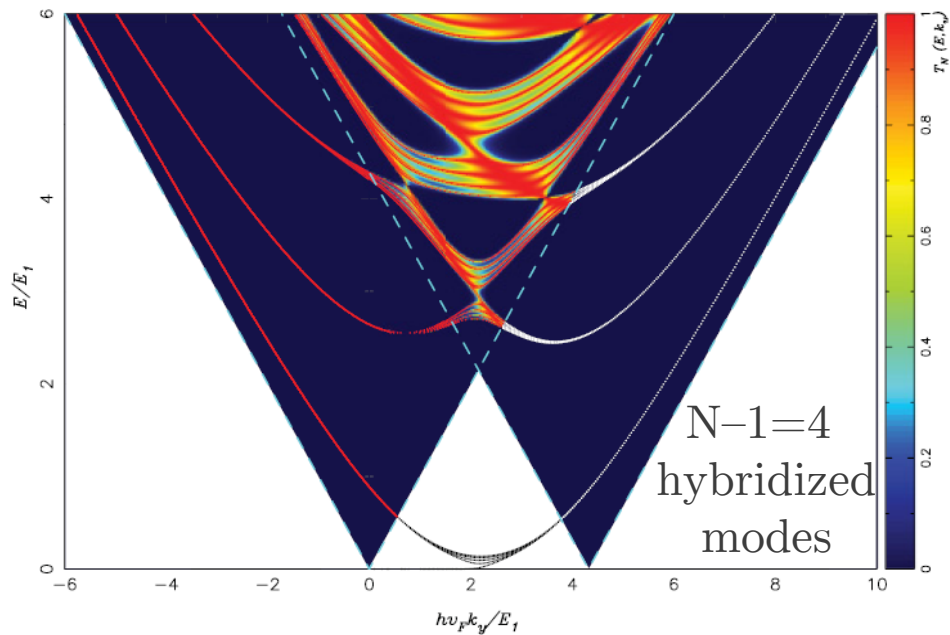
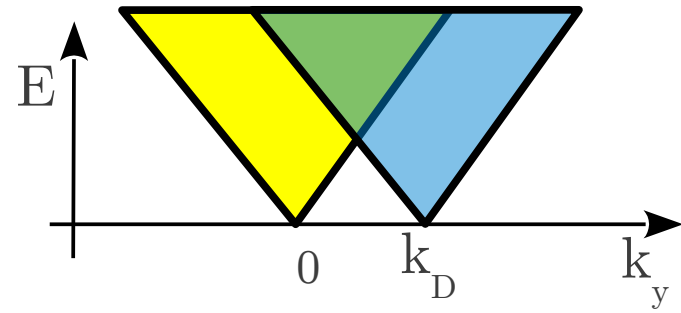


FIG. 3. (Color online) Single-electron transmission  $T_5(E, k_y)$ , Eq. (5) across a superlattice of  $N = 5$  identical barriers (Fig. 1), as a function of scaled transverse wave vector  $\hbar v_F k_y / E_1$  and scaled energy  $E / E_1$ , Eq. (6). All other parameters are as in Fig. 2. Red lines outside the right cone correspond to resonant modes.

# $N=5$ “barriers”: minibands, and hybridization of bound states

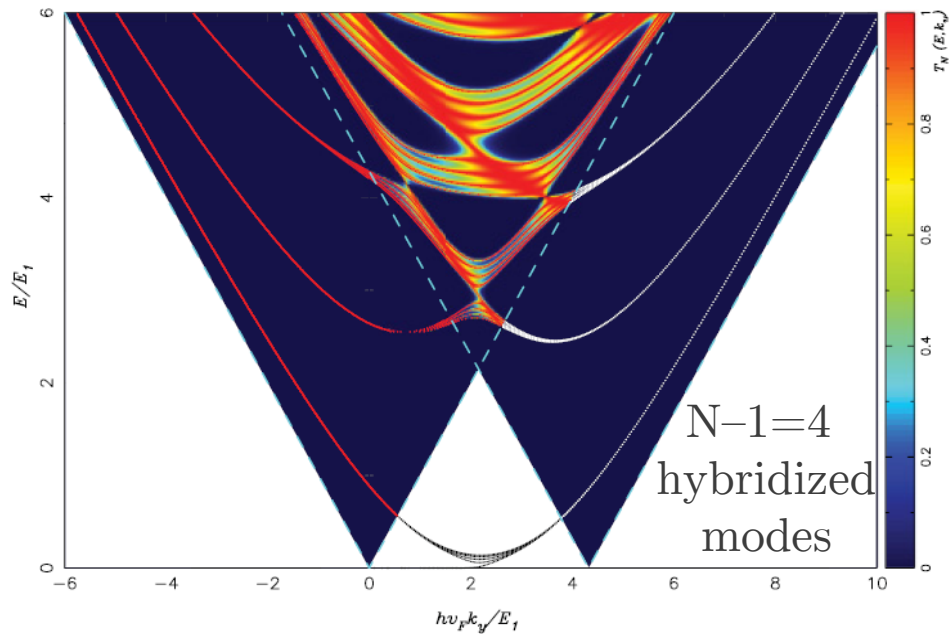
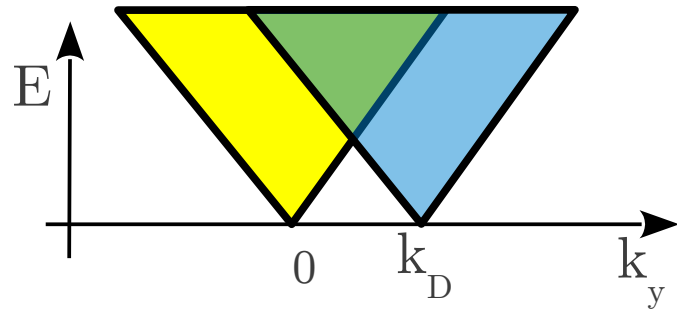
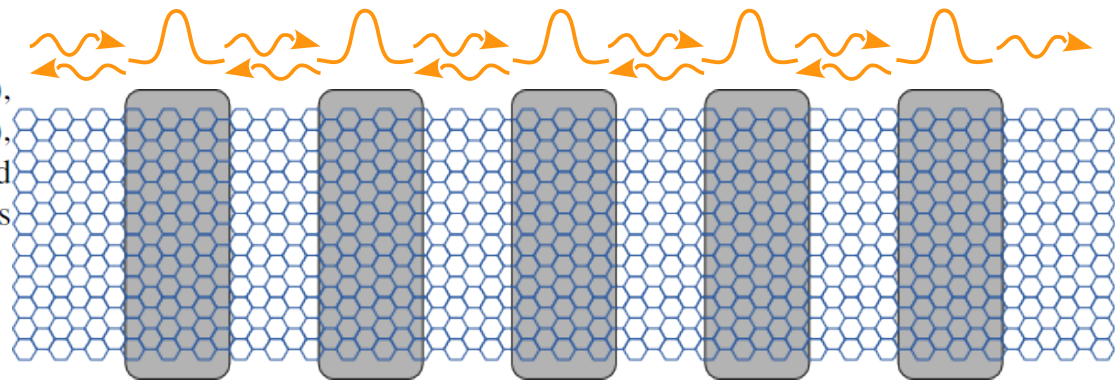


FIG. 3. (Color online) Single-electron transmission  $T_5(E, k_y)$ , Eq. (5) across a superlattice of  $N = 5$  identical barriers (Fig. 1), as a function of scaled transverse wave vector  $\hbar v_F k_y / E_1$  and scaled energy  $E / E_1$ , Eq. (6). All other parameters are as in Fig. 2. Red lines outside the right cone correspond to resonant modes.



# $N=5$ “barriers”: minibands, and hybridization of bound states

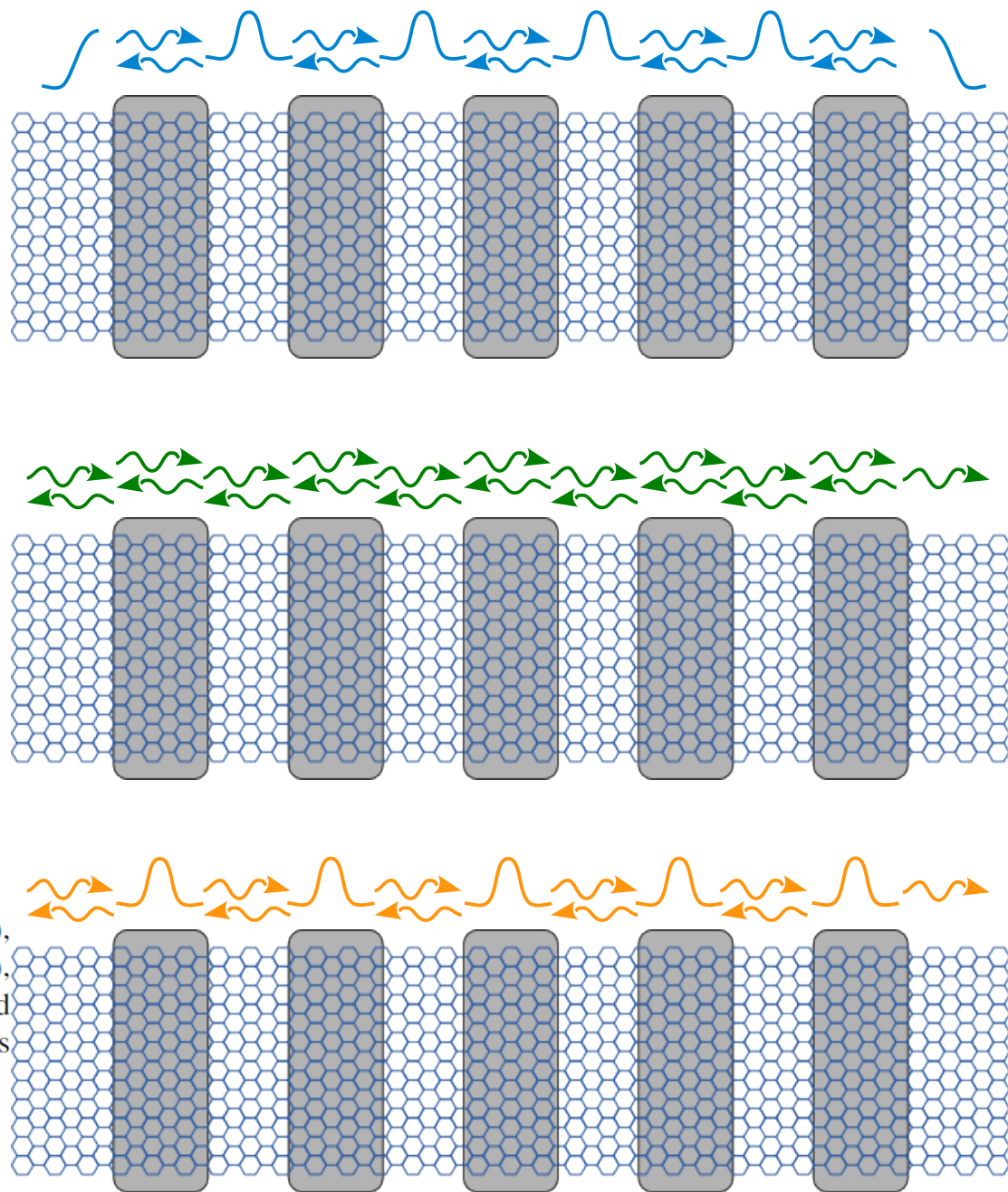
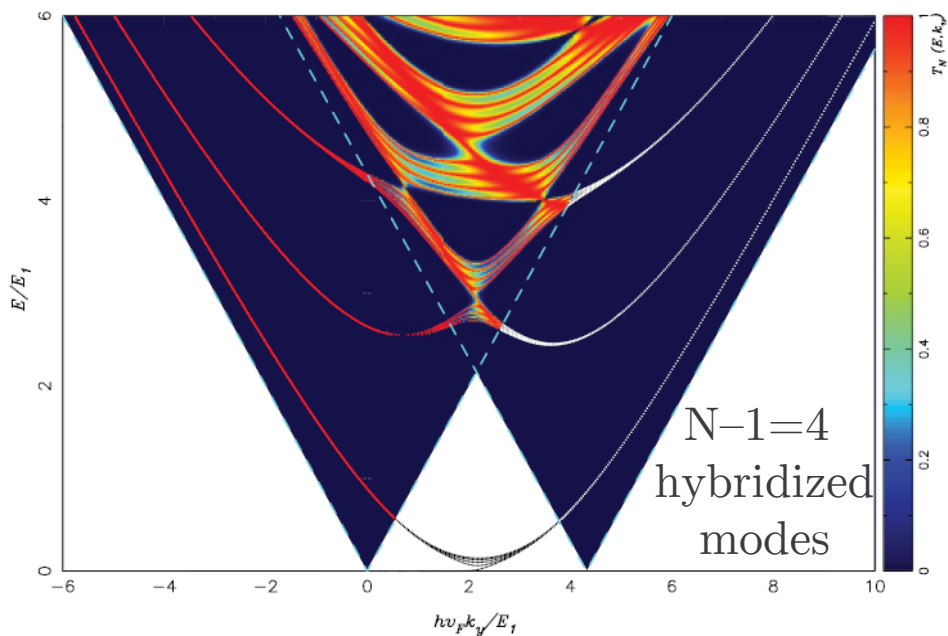
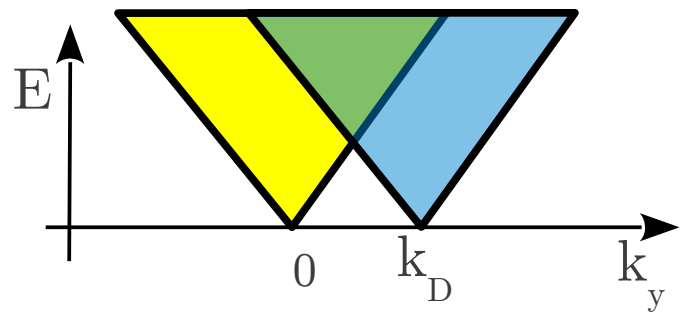


FIG. 3. (Color online) Single-electron transmission  $T_5(E, k_y)$ , Eq. (5) across a superlattice of  $N = 5$  identical barriers (Fig. 1), as a function of scaled transverse wave vector  $\hbar v_F k_y / E_1$  and scaled energy  $E / E_1$ , Eq. (6). All other parameters are as in Fig. 2. Red lines outside the right cone correspond to resonant modes.

## Resonant modes in strain-induced graphene superlattices

F. M. D. Pellegrino,<sup>1,2</sup> G. G. N. Angilella,<sup>1,2,3,4</sup> and R. Pucci<sup>1,2</sup>

<sup>1</sup>*Dipartimento di Fisica e Astronomia, Università di Catania, Via S. Sofia, 64, I-95123 Catania, Italy*

<sup>2</sup>*CNISM, UdR di Catania, I-95123 Catania, Italy*

<sup>3</sup>*Scuola Superiore di Catania, Università di Catania, Via Valdisavoia, 9, I-95123 Catania, Italy*

<sup>4</sup>*INFN, Sezione di Catania, I-95123 Catania, Italy*

(Received 20 March 2012; published 7 May 2012)

- “strain-induced graphene superlattices can accommodate additional resonant quasiparticles”
  - misleading: resonances occur due to modulation of the “finite- $k_y$  gap”.
  - Not a peculiarity of strain effects;
- Bound states;
- “We thus surmise that a strain-induced superlattice in graphene can be used as a filter for the resonant modes discussed here.”
- Their previous paper: PRB **84**, 195404 (2011)
  - “Transport properties of graphene across strain-induced nonuniform velocity profiles”
    - Low energy Hamiltonian for strained graphene;
    - Deformation of Dirac cone = same order as the shift in k-space;

# Chebyshev identity: $N$ th power of a $2 \times 2$ matrix

[Griffiths and Steinke, Am. J. Phys. **69** (2), 137 (2001)]

- Characteristic equation for matrix  $\mathbf{P}$ :  $p^2 - p \operatorname{Tr}(\mathbf{P}) + \det(\mathbf{P}) = 0$

- Replace eigenvalues by the matrix itself:  $\mathbf{P}^2 - 2\mathbf{P}\xi + \mathbf{I} = 0$        $\xi \equiv \frac{1}{2}\operatorname{Tr}(\mathbf{P})$   
(Cayley-Hamilton theorem)

- Recursion relation:  $\mathbf{P}^N = \mathbf{P}U_{N-1}(\xi) - \mathbf{I}U_{N-2}(\xi)$   
Task: find polynomial  $U$

- Multiply by  $\mathbf{P}$ :  $\mathbf{P}^{N+1} = \mathbf{P}^2 U_{N-1}(\xi) - \mathbf{P}U_{N-2}(\xi)$

- $N \rightarrow N+1$  in  $\mathbf{P}^N$ :  
$$\left\{ \begin{array}{l} \mathbf{P}^{N+1} = (2\mathbf{P}\xi - \mathbf{I})U_{N-1}(\xi) - \mathbf{P}U_{N-2}(\xi) \\ \mathbf{P}^{N+1} = \mathbf{P}U_N(\xi) - \mathbf{I}U_{N-1}(\xi) \end{array} \right.$$

- Recursion relation for Chebyshev polynomials:  $U_{N+2}(\xi) - 2\xi U_{N+1}(\xi) + U_N(\xi) = 0$

$$U_N(\xi) = \frac{\sin(N+1)\gamma}{\sin\gamma}$$

$$\mathbf{P}^N = \mathbf{P}U_{N-1}(\xi) - \mathbf{I}U_{N-2}(\xi)$$